Multiscale study of the structure and mechanical properties of dentin

Asef HEMMATI[a,b], **Thomas REISS**[a], **Nicolas SCHMITT**[b,c], **Elsa VENNAT**[a,d]

(a) MSSMat, CentraleSupélec, Université Paris-Saclay, 3 rue Joliot Curie, 91 190 Gif-sur-Yvette, France
(b) LMT, ENS Paris-Saclay, Université Paris-Saclay, 61 avenue du Président Wilson 94 235 Cachan Cedex, France
(c) ESPE, Université Paris-Est Créteil, Université Paris-Est, Place du 8 Mai 1945, 93 203 Saint-Denis Cedex, France
(d) URB2i, Université Paris-Descartes, Université Sorbonne Paris Cité, 1 rue Maurice Arnoux, 92120 Montrouge, France

Summary

There is no consensus on the acceptable range of the mechanical properties of dentin, the main tissue of the tooth. It is probably due to the lack of knowledge of the geometric characteristics of the microstructure (e.g., tubules orientation) and the nanostructure and in the local variation in the properties at these scales. In this paper, we show some results from a study on the morphology of dentin at different scales that will be the basis for numerical simulation of dentin mechanical behavior.

Keywords: Dentin; Scanning Electron Microscopy (SEM); Focused Ion Beam (FIB); Image analysis; Microcompression test;

1. Introduction

At the microscale, dentin is a composite made of irregular hollow cylinders -internal diameter ≈1 µm, called *tubules*- embedded in a matrix of *InterTubular Dentin* (ITD) (Fig. 1.a). The space inside a tubule is called *lumen* and is initially filled with liquid. The cuff surrounding the lumen is made of *PeriTubular Dentin* (PTD), which is hypermineralized and collagen-poor and stiffer than the IDT (Pashley 1996).

Modeling the tubules by idealized hollow cylinders (Fig. 2b) provides the dentin transverse isotropic properties (Kinney et al. 2003). But this anisotropy may not be detected by mechanical test performed on a few millimeter size sample, because the tubule orientation changes up to 90 degrees in a distance of 2-3 millimeters (Fig. 3c).

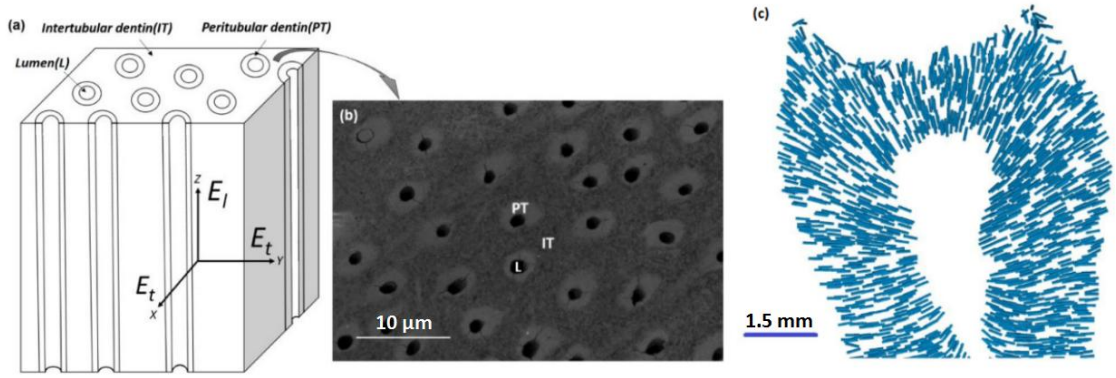

Figure 1: ***(a)*** *The simplified geometry of dentin at microscale naming its constituents, adapted from Wang et al. 2015* ***(b)*** *SEM image of dentin, adapted from Wang et al. 2015* ***(c)*** *The variation of tubule orientation in dentin revealed with X-ray tensor tomography, adapted from Jud et al. 2016*

At the nanoscale, the intertubular dentin is mostly made of type I collagen fibrils, –diameter ≈100 nm after Bertassoni et al. 2012- mineralized by hydroxyapatite crystals. The organization of collagen fibrils is believed to confer anisotropy to both elastic (Kinney et al. 2003) and inelastic properties of dentin (Nalla et al. 2002, Rasmussen and Patchin 1984).

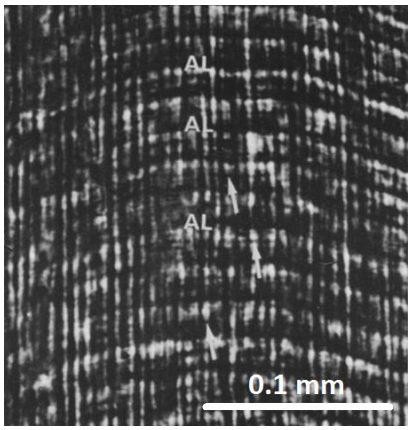

Figure 2: Incremental lines (curvy and horizontal) at right angles to the dentinal tubules (vertical) in the crown dentin, stained with silver. According to Chowdhary and Reddy (2010), the right angle implies that the dentin is from an adult. The most visible lines are called Andresen-Von Ebner lines. They are approximately 20 µm away from each other and represent the 5-day period of dentin growth, at the beginning and the end of which the collagen matrix has the same orientation. The lines in between are the daily incremental lines, adapted from Kawasaki et al. 1979.

Close to the *enamel* -the substance of the crown covering the dentin-, the collagen fibrils stand perpendicular to the *Dentino-Enamel Junction* (DEJ) (Nanci 2012) and parallel to the long axis of tubules (Elbaum et al. 2007). Some of them – 80-120 nm in diameter, called von Korff fibers- even penetrate the enamel (Zaslansky 2008).

Apart from this thin layer, collagen fibrils lie in *incremental planes* that are traces of dentin layer-by-layer mineralization. As shown in figure 2, they are perpendicular to tubules. The organization of fibrils in those planes depends on the location in dentin.

One way to evaluate the mechanical properties of the complex hierarchical dentin microstructure described previously consists in estimating the effective properties by homogenization techniques, sometimes applied at several scales (Qin and Swain 2004, Jeanneret et al. 2017, Guo and Gao 2006).

What seems to be unexplored yet, is simulating dentin at nano and microscales with more realistic structures. To visualize them, techniques like SEM and serial sectioning (by FIB-SEM) are used. First results will be shown below. These techniques can deliver images with unprecedented details so that it will be possible in the future to simulate accurately the mechanical response of the dentin by accounting refined details on the true microstructure of the dental tissue.

2. Materials and methods

A human third molar was taken and disinfected by chloramine-T solution (0.5%). Then it was kept in Ringer's solution (¼ strength) and cut by Diamond saw before being dried in ascending ethanol series. The sample was bathed in alcohol of 25%, 50%, 75% and 95% volume, for 20 minutes each. The procedure was completed by two 10-minute bathes in absolute alcohol during 12 hours. Between each two steps the sample was cleaned by supersonic bath.

2D SEM imaging was performed at MSSMat laboratory with FEI Helios NanoLab 660 using the Backscattered electrons (BSE) detector to improve the contrast between the peritubular dentin and

the intertubular dentin. The software MAPS from FEI was used to map a large area of dentin through the acquisition of a stack of BSE images.

3D imaging was also performed. An area of the studied tooth (surface ≈ 15x24 µm^2) was selected. This area was subsequently imaged by electron beam and carved by focused ion beam (FIB-SEM). These steps were repeated until a depth of ≈ 12.8 µm. A stack of 535 images was acquired and the cropped 3D image reconstructs a volume of ≈15×16×13 µm^3.

2D and 3D images were analyzed using the softwares ImageJ (Schneider et al. 2012) and MATLAB (MATLAB 2018) to study the micromorphology of dentin. The main challenge was to segment hundreds of grayscale images of microstructure areas into the constituents of the dentin. The tool used here was Weka trainable segmentation that works by machine learning (Arganda-Carreras et al., 2017). It recognizes the common characteristics of the input zones that the user has chosen separately from each constituent. Then it classifies the whole image (or stack of images) into classes, each representing one constituent. The following classes were selected: lumen, PTD and ITD.

3. Results and discussion

It is generally known that close to dentino-enamel junction (DEJ), dentin has a higher portion of intertubular dentin ITD and its tubules have smaller internal and external diameters. Wang (2016) has measured the area fraction of dentin constituents along rectangular dentin samples using SEM images, reaching the same conclusion. But in his study, the exact distance from the DEJ was not measured. Here, this effect was quantified by measuring the diameters and area fractions of the constituents by segmenting the images (which make up the map) as explained above and their distances from DEJ. To measure the distance of an image to the DEJ, the center of each image in the map was assumed to be closer to the junction in the cutting plane than in other planes (Fig. 3.b).

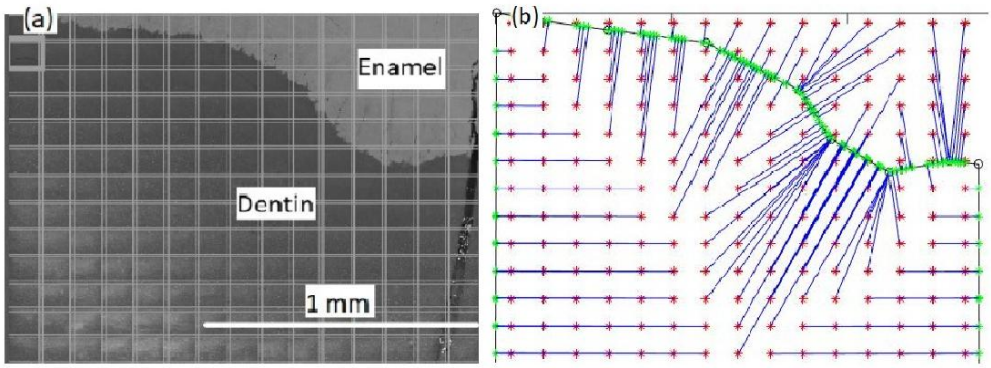

*Figure 3: **(a)** Map of tooth cross section. Each rectangle represents a SEM image of ≈127x110 µm² **(b)** MATLAB code "distance2curve" was used to measure the distance (blue lines) between the center of each image (red stars) and the DEJ. The horizontal lines belong to the images that are closer to the borders of the map than to the junction*

Figures 4.a and 4.b demonstrate the results.

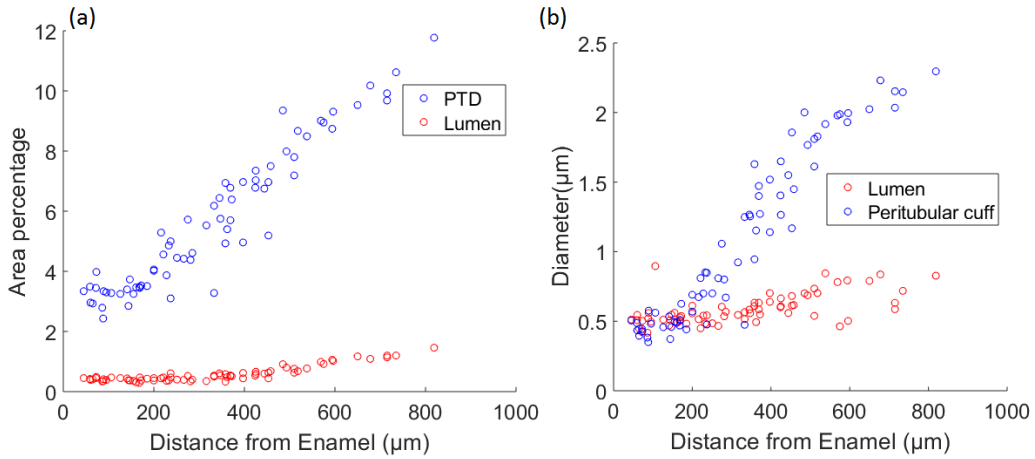

*Figure 4: **(a)** Area fraction of lumen and peritubular dentin versus distance from enamel **(b)** Mean diameter of lumen and peritubular dentin (PTD) versus distance from enamel*

Mjör and Nordahl (1996) have studied the branching of dentinal tubules and used the term *fine branches* for those having an internal diameter of 0.3-0.7 µm. They were aware of the peritubular cuff around these fine branches but did not quantify them. Vennat et al. (2017) have modeled fine branches -without their peritubular cuffs-. They suggest that they have a negative effect on the dentin mechanical properties as they lead to stress concentration.

Including peritubular cuffs in the simulation of fine branches needs data on their shape. We did a particle analysis on the segmented 2D images of fine branches. In ImageJ, "Analyze particle" fits ellipses on the tubules. The minor diameter of each ellipse was taken to be the diameter of the idealized cylinder. The mean ratio of the external to internal diameter of fine branches is 2.8 (n=95, SD 1.1).

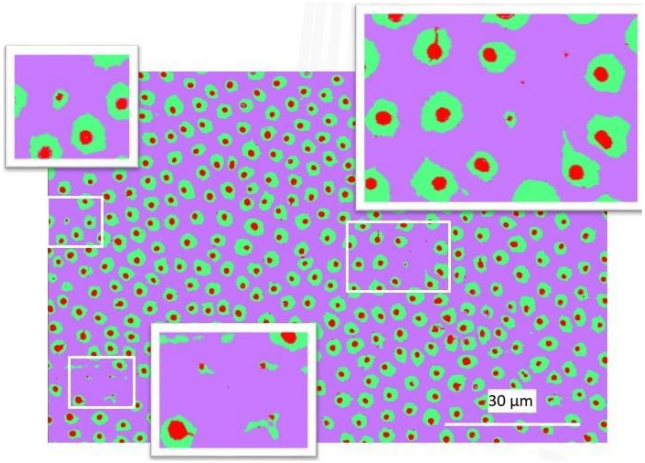

Figure 5: A SEM image of dentin (≈1.3 mm from enamel) segmented into lumen (red), PTD (green) and ITD (purple), magnified sections include fine branches

The segmentation method described above was also used to segment the stack of images achieved by FIB-SEM. Some results will be shown during the presentation.

4. Conclusion and perspectives

A methodology has been developed to characterize the main features of the structure of dentin at different scales. The first results are encouraging and will permit to conduct an in-depth investigation of the complex hierarchical structure of dentin. In the future microcompression tests

will be performed on small samples of dentin to investigate the mechanical properties of the RVE. We expect a substantial contribution to the mechanical characterization of dentin by developing a specific tool combining imaging of the dentin structure, mechanical tests and simulations of the reconstructed microstructure at macroscale.

5. References

1. Arganda-Carreras, I., Kaynig, V., Rueden, C., Eliceiri, K. W., Schindelin, J., Cardona, A., Sebastian Seung, H. (2017). Trainable Weka Segmentation: a machine learning tool for microscopy pixel classification. *Bioinformatics*, 33(15), 2424-2426.
2. Bertassoni, L. E., Orgel, J. P., Antipova, O., Swain, M. V. *(2012).* The dentin organic matrix–limitations of restorative dentistry hidden on the nanometer scale. *Acta Biomaterialia*, 8(7), 2419-2433.
3. Chowdhary, N., Reddy, V. S. (2010). Dentin comparison in primary and permanent molars under transmitted and polarized light microscopy: an in vitro study. *Journal of Indian Society of Pedodontics and Preventive Dentistry*, 28(3), 167-172.
4. D'Errico, J. (2005). Distance2curve (https://fr.mathworks.com/matlabcentral/fileexchange/34869-distance2curve), MATLAB Central File Exchange. Retrieved December 7, 2018.
5. Elbaum, R., Tal, E., Perets, A. I., Oron, D., Ziskind, D., Silberberg, Y., Wagner, H. D. (2007). Dentin micro-architecture using harmonic generation microscopy. *Journal of dentistry*, 35(2), 150-155.
6. Guo, X., Gao, H. (2006). Bio-inspired material design and optimization. *Proc. IUTAM Symposium on Topological Design Optimization of Structures, Machines and Materials* (pp. 439-453). Springer, Dordrecht.
7. Hashin, Z., Rosen, B. W. (1964). The elastic moduli of fiber-reinforced materials. *Journal of Applied Mechanics*, 31(2), 223-232.
8. Jeanneret, R., Arson, C., Vennat, E. (2017). Homogenization of dentin elastic properties based on microstructure characterization, statistical back-analysis, and FEM simulation. *Proc. Poromechanics VI*, 1339-1346.
9. Kawasaki, K., Tanaka, S., Ishikawa, T. (1979). On the daily incremental lines in human dentine. *Archives of Oral Biology*, 24(12), 939-943.
10. Kinney, J. H., Pople, J. A., Marshall, G. W., & Marshall, S. J. (2001). Collagen orientation and crystallite size in human dentin: a small angle X-ray scattering study. *Calcified Tissue International*, 69(1), 31-37.
11. Kinney, J. H., Marshall, S. J., & Marshall, G. W. (2003). The mechanical properties of human dentin: a critical review and re-evaluation of the dental literature. *Critical Reviews in Oral Biology & Medicine*, 14(1), 13-29.
12. MATLAB R2018a (2018), Natick, Massachusetts, The MathWorks Inc.
13. Mjör, I. A., & Nordahl, I. (1996). The density and branching of dentinal tubules in human teeth. *Archives of Oral Biology*, 41(5), 401-412.
14. Nalla, R. K., Kinney, J. H., & Ritchie, R. O. (2003). Effect of orientation on the in vitro fracture toughness of dentin: the role of toughening mechanisms. *Biomaterials*, *24*(22), 3955-3968.
15. Nanci, A. (2012). *Ten cate's oral histology development, structure, and function, 8/e*. Elsevier India.
16. Pashley, D. H. (1996). Dynamics of the pulpo-dentin complex. *Critical Reviews in Oral Biology & Medicine*, *7*(2), 104-133.
17. Pashley, D. H., Zhang, Y., Agee, K. A., Rouse, C. J., Carvalho, R. M., & Russell, C. M. (2000). Permeability of demineralized dentin to HEMA. *Dental Materials*, 16(1), 7-14.
18. Qin, Q. H., & Swain, M. V. (2004). A micro-mechanics model of dentin mechanical properties. *Biomaterials*, 25(20), 5081-5090.
19. Rasmussen, S. T., & Patchin, R. E. (1984). Fracture properties of human enamel and dentin in an aqueous environment. *Journal of Dental Research*, 63(12), 1362-1368.
20. Schneider C.A., Rasband, W.S., Eliceiri, K.W. (2012). NIH Image to ImageJ: 25 years of image analysis. *Nature Methods*, 9, 671-675.
21. Vennat, E., Wang, W., Genthial, R., David, B., Dursun, E., Gourrier, A. (2017). Mesoscale porosity at the dentin-enamel junction could affect the biomechanical properties of teeth. *Acta biomaterialia*, 51, 418-432.
22. Wang, W. (2016). *Caractérisation géométrique et mécanique multi-échelle de la dentine humaine*. PhD dissertation, University Paris-Saclay. Retrieved from https://tel.archives-ouvertes.fr/
23. Zaslansky, P. (2008) Collagen: structure and mechanics, an introduction. In Collagen (pp. 421-442). In Fratzl, P. (Ed.), Springer, Boston, MA.